Geotech Geol Eng (2010) 28:525–531
DOI 10.1007/s10706-010-9327-3

TECHNICAL NOTE

Seismic Passive Earth Thrust on Retaining Walls with Cohesive Backfills Using Pseudo-Dynamic Approach

A. H. Shafiee · A. Eskandarinejad · M. Jahanandish

Received: 10 January 2010 / Accepted: 1 April 2010 / Published online: 13 April 2010

Abstract In this paper, the pseudo-dynamic approach is used to estimate seismic passive earth thrust on retaining walls with cohesive-frictional backfills. The time-dependent pseudo-dynamic approach considers the influence of dynamic parameters such as the velocity of primary and shear waves, the period of lateral shaking, and the phase and amplitude variations of horizontal and vertical earthquake accelerations with depth. The failure plane behind the wall is assumed to be planar. The analysis is based on the equilibrium of forces which act within the failure wedge. The obtained results show that the backfill cohesion increases both the seismic passive earth thrust and the failure plane inclination angle with the horizontal plane. It is also observed that both horizontal and vertical seismic accelerations have decreasing effect on seismic passive earth thrust as well as failure plane inclination angle. The results of present pseudo-dynamic analysis propose a lower solution for seismic passive earth thrust compared to earlier pseudo-static solution available in the literature.

A. H. Shafiee (✉) · M. Jahanandish
Civil Engineering Department, Shiraz University, Shiraz, Iran
e-mail: shafiee.amirhossein@gmail.com

M. Jahanandish
e-mail: jahanand@shirazu.ac.ir

A. Eskandarinejad
Civil Engineering Department, University of Hormozgan, Bandarabbas, Iran
e-mail: alireza.eskandarinejad@yahoo.com

Keywords Seismic passive earth thrust · Retaining walls · Pseudo-dynamic approach · Cohesive backfill

1 Introduction

The estimation of seismic passive earth pressure is vital in design of safe retaining walls. The majority of available solutions in the literature consider the backfill soil to be cohesionless (Soubra 2000; Kumar 2001; Ghahramani and Anvar 2004). The pioneering studies belong to Okabe (1926) and Mononobe and Matsuo (1929) who used the limit equilibrium method and a planar failure surface to compute seismic earth pressure coefficients. Their solution is known as Mononobe-Okabe method. However, a retaining wall may be built to support a cohesive-frictional backfill in practice. Thus, it is very essential to compute seismic earth resistance on such walls. The number of investigations that determine the seismic passive earth pressure on retaining walls with cohesive-frictional backfills is limited. The reason seems to be due to complex equations and cumbersome computational effort when backfill cohesion and the wall adhesion are taken into account. Saran and Prakash (1968) and Saran and Gupta (2003) extended the Mononbe-Okabe solution to walls with c-φ soil backfill. They obtained different failure planes for a unique soil, wall and earthquake conditions which is not compatible with practical situations. Richards and Shi (1994) presented a solution based on elastic–plastic analysis for seismic stresses of a Mohr–Coulomb soil with cohesion. All of the mentioned studies applied the pseudo-static method to estimate seismic earth resistance. The pseudo-static method is time-independent and could not consider the real dynamic nature of earthquake acceleration. In order to remove this deficiency, Steedman and Zeng (1990) introduced a time-dependent approach (later called pseudo-dynamic approach) for seismic loading. In the pseudo-dynamic approach, the influence of dynamic parameters such as the velocity of body waves, the period of lateral shaking, and the phase and amplitude variation of horizontal and vertical earthquake accelerations with depth is taken into account. The pseudo-dynamic approach was extended by Choudhury and Nimbalkar (2005) who computed seismic passive earth pressure on retaining walls with cohesionless backfills.

In the present paper, the pseudo-dynamic approach is used to compute seismic passive earth thrust on vertical retaining walls with cohesive backfills for a wide range of friction angles and horizontal and vertical earthquake accelerations. In other words, this study is an extension of Choudhury and Nimbalkar (2005) research by considering the backfill soil cohesion, amplification of earthquake acceleration with depth, and variations in shear and primary waves velocities. The results are presented in charts and compared to available solutions in the literature.

2 Problem Definition

As shown in Fig. 1, the problem consists of a rigid vertical retaining wall AB of height H with a c-φ soil backfill. The following assumptions are made in the present analysis:

1. The weight of the retaining wall is negligible compared to the weight of the failure wedge. Thus, the weight of the wall is not considered in the analysis.
2. The failure surface (BD) behind the wall is planar with the inclination angle (α) with the horizontal plane. The assumption of planar failure surface has been widely used in the literature because of its simplicity and its' relatively acceptable results. The aim of the present research is not to consider complex failure planes, as our equations are complicated enough, but rather to investigate the application of pseudo-dynamic approach to compute the seismic passive force on retaining walls with cohesive backfills.
3. Both the primary wave velocity (V_p) and shear wave velocity (V_s) propagate through the backfill layer as a result of earthquake loading in the direction shown in Fig. 1. Das (1993) pointed out that the ratio of V_p/V_s is equal to 1.87 for most of geological materials.
4. The backfill soil is completely dry and no pore water pressure or water flow exists in the backfill. The influence of drainage in the backfill soil is out of the scope of this study.

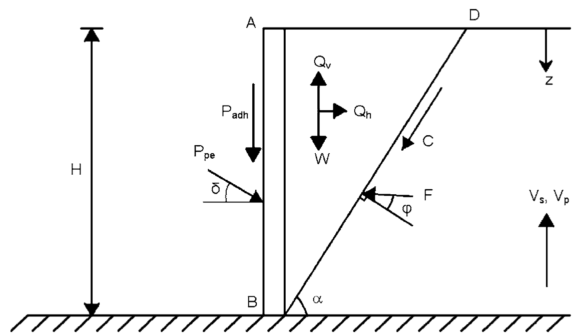

Fig. 1 Model retaining wall and associated forces

In Fig. 1, W is the weight of the failure wedge; Q_h and Q_v are total horizontal and vertical inertia forces within the failure wedge ABD, respectively; F is the resultant of frictional forces acting on the failure plane; C is the total cohesive force along the failure plane; P_{adh} is the adhesive force equal to $cH \tan\delta/\tan\varphi$ where δ is the wall friction angle and P_{pe} is the total passive thrust (force).

In the following of this paper, first the method of analysis is discussed in details in Sect. 3, and then the results of analysis are presented in Sect. 4 and compared to the available solution in the literature in Sect. 5. At last, the conclusion is presented in Sect. 6.

3 Method of Analysis

The pseudo-dynamic approach considers uniform sinusoidal horizontal and vertical accelerations with amplitudes of a_h and a_v, respectively, and the period of lateral shaking T at any depth z and time t as follows:

$$\alpha_h(z,t) = \left[1 + \frac{(H-z)}{H}(f_a - 1)\right]\alpha_h g \sin\omega\left(t - \frac{H-z}{V_s}\right) \quad (1)$$

$$\alpha_v(z,t) = \left[1 + \frac{(H-z)}{H}(f_a - 1)\right]\alpha_v g \sin\omega\left(t - \frac{H-z}{V_p}\right) \quad (2)$$

where f_a is the amplification factor, i.e., it designates the variation of shaking amplitude with depth and $\omega = 2\pi/T$ is the angular frequency of lateral shaking.

The weight of the failure wedge ABD is given by:

$$W = 0.5\gamma H^2 \cot(\alpha) \quad (3)$$

The total cohesive force (C) along the failure plane BD can be expressed by:

$$C = cH/\sin\alpha \quad (4)$$

By computing the inertia force on an element of thickness dz in the failure wedge, and then integrating over depth (z), Choudhury and Nimbalkar (2007) derived the following expression for total horizontal inertia force on the failure wedge ABD:

$$Q_h(t) = \frac{\lambda\gamma a_h}{4\pi^2\tan\alpha}[2\pi H\cos\omega\xi + \lambda(\sin\omega\xi - \sin\omega t)] + \frac{\lambda\gamma a_h(f_a-1)}{4\pi^3 H\tan\alpha}[2\pi H(\pi H\cos\omega\xi + \lambda\sin\omega\xi) + \lambda^2(\cos\omega t - \cos\omega\xi)] \quad (5)$$

and the following expression for total vertical inertia force:

$$Q_v(t) = \frac{\eta\gamma a_v}{4\pi^2\tan\alpha}[2\pi H\cos\omega\psi + \eta(\sin\omega\psi - \sin\omega t)] + \frac{\eta\gamma a_v(f_a-1)}{4\pi^3 H\tan\alpha}[2\pi H(\pi H\cos\omega\psi + \eta\sin\omega\psi) + \eta^2(\cos\omega t - \cos\omega\psi)] \quad (6)$$

where $\lambda = TV_s$, $\eta = TV_p$ are the wave lengths of shear and primary waves, respectively and $\xi = t - H/V_s$, $\psi = t - H/V_p$.

Equilibrium of forces in the horizontal direction $[\rightarrow +]$ yields:

$$P_{pe}\cos\delta - cH\cot\alpha + Q_h - F\sin(\alpha+\varphi) = 0$$

or

$$F = \frac{P_{pe}\cos\delta - cH\cot\alpha + Q_h}{\sin(\alpha+\varphi)} \quad (7)$$

Equilibrium of forces in the vertical direction $[\downarrow +]$ gives:

$$W + P_{pe}\sin\delta + P_{adh} - Q_v + cH - F\cos(\alpha+\varphi) = 0 \quad (8)$$

Substituting Eq. (7) into Eq. (8) and following some simplifications yields:

$$P_{pe} = \frac{W\sin(\alpha+\varphi) - Q_h\cos(\alpha+\varphi) - Q_v\sin(\alpha+\varphi) + cH[\sin(\alpha+\varphi)(1+\tan\delta/\tan\varphi) + \cos(\alpha+\varphi)\cot\alpha]}{\cos(\alpha+\varphi+\delta)} \quad (9)$$

In this type of problem, it is a common practice to present the solutions in a nondimensional form as $P^*_{pe} = P_{pe}/\gamma H^2$ and $c^* = c/\gamma H$. Thus, Eq. (9) can be rewritten as follows:

$$P^*_{pe} = \frac{\frac{1}{\gamma H^2}[W\sin(\alpha+\varphi) - Q_h\cos(\alpha+\varphi) - Q_v\sin(\alpha+\varphi)] + c^*[\sin(\alpha+\varphi)(1+\tan\delta/\tan\varphi) + \cos(\alpha+\varphi)\cot\alpha]}{\cos(\alpha+\varphi+\delta)} \quad (10)$$

For the case of fully smooth wall ($\delta = 0.0$), having substituted Eqs. (3), (5), (6) into Eq. (10), P^*_{pe} can be obtained by:

$$P^*_{pe} = \frac{\tan(\alpha+\varphi)}{2\tan\alpha} - \frac{1}{8\pi^3\tan\alpha}\{[\left(\frac{\lambda}{H}\right)x_1 + \left(\frac{\lambda}{H}\right)^2 x_2 - \left(\frac{\lambda}{H}\right)^3 x_3]a_h + [(\frac{\eta}{H})y_1 + (\frac{\eta}{H})^2 y_2 - (\frac{\eta}{H})^3 y_3]a_v\tan(\alpha+\varphi)\} + c^*[\tan(\alpha+\varphi) + \cot\alpha] \quad (11)$$

where

$$x_1 = 4\pi^2 f_a \cos 2\pi(\frac{t}{T} - \frac{H}{\lambda})$$
$$x_2 = 2\pi[(2f_a - 1)\sin 2\pi(\frac{t}{T} - \frac{H}{\lambda}) - \sin 2\pi(\frac{t}{T})]$$
$$x_3 = 2(f_a - 1)[\cos 2\pi(\frac{t}{T} - \frac{H}{\lambda}) - \cos 2\pi(\frac{t}{T})]$$
$$y_1 = 4\pi^2 f_a \cos 2\pi(\frac{t}{T} - \frac{H}{\eta})$$
$$y_2 = 2\pi[(2f_a - 1)\sin 2\pi(\frac{t}{T} - \frac{H}{\eta}) - \sin 2\pi(\frac{t}{T})]$$
$$y_3 = 2(f_a - 1)[\cos 2\pi(\frac{t}{T} - \frac{H}{\eta}) - \cos 2\pi(\frac{t}{T})]$$

The last term in Eq. (11) is that part of total passive force corresponds to backfill cohesion. It can be noticed in Eq. (10) that P^*_{pe} is a function of α, t/T, H/λ, and H/η. H/λ is the ratio of time needed for shear waves to pass through the wall height to the period of lateral shaking (T), and H/η is the ratio of time needed for primary waves to pass through the wall height to the period of lateral shaking (T). In the present investigation, the analyses were carried out for $H/\lambda = 0.3$, 0.4, 0.5, 0.6 and $H/\eta = 0.16$, 0.21, 0.27, 0.32, respectively. The minimum value of P^*_{pe} should be obtained by optimizing Eq. (10) with respect to α and t/T. The results of present computations are shown in the next section.

4 Results

The computations were carried out for $\varphi = 5$–$50°$, $\delta = 0.0$, $0.5\ \varphi$, φ, $a_h = 0$–0.5, $a_v = 0$, $0.5a_h$, a_h, $c^* = 0$, 0.05, 0.1, 0.2, and $f_a = 1$, 1.2, 1.4, 1.6, 1.8, 2. It should be mentioned that because of the complexity of Eqs. (5)–(11), the main computations of this study are allocated to $\delta = 0.0$ case. Albeit, the effect of wall friction angle and adhesion on total passive force is shown in a separate table. Similarly to Shukla et al. (2009), the upper limit for horizontal seismic coefficient $\alpha_{h(cr)}$, is taken equal to:

$$\alpha_{h(cr)} = (1 - \alpha_v)\tan\varphi + 2c^* \tag{12}$$

Figure 2 shows the variation of nondimensional total passive force (P^*_{pe}) with horizontal seismic coefficient (α_h) for $c^* = 0.05$, $\varphi = 10$, 20°, 30°, $\delta = 0.0$, $\alpha_v = 0$, $0.5\alpha_h$, α_h, $H/\lambda = 0.3$ and $H/\eta = 0.16$. It is seen that the total passive force decreases with increase in both α_h and α_v. This decreasing effect is in fact due to the negative signs of horizontal and vertical inertia forces (Q_h, Q_v, respectively) in Eq. (10). Figure 2 also depicts that the influence of α_v is more significant for higher values of α_h.

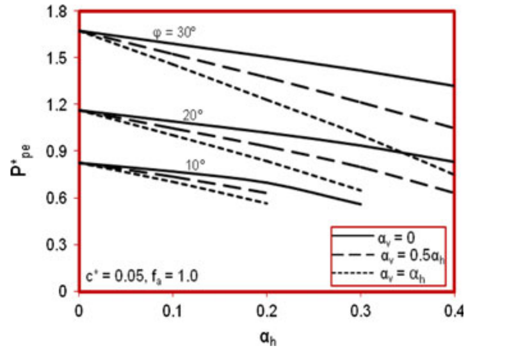

Fig. 2 Variation of nondimensional total passive force (P^*_{pe}) with horizontal seismic coefficient (α_h) for $c^* = 0.05$, $\varphi = 10°$, 20°, 30°, $\delta = 0.0$, $\alpha_v = 0$, $0.5\ \alpha_h$, α_h, $H/\lambda = 0.3$ and $H/\eta = 0.16$

The variation of P^*_{pe} with c^* for different values of friction angle (φ) and $\delta = 0.0$, $\alpha_h = 0.1$, $\alpha_v = 0.5\alpha_h$, $H/\lambda = 0.3$ and $H/\eta = 0.16$ is shown in Fig. 3. It is observed that c^* has an increasing effect on P^*_{pe}. The reason of this increase is the positive sign of cohesion in Eq. (10). In other words, the backfill soil cohesion improves the shear resistance of the backfill layer and therefore, a greater force is required to induce the passive failure. Figure 3 also depicts that P^*_{pe} is greater for higher friction angles and as nondimensional cohesion (c^*) increases, the curves corresponding to different friction angles move away from each other.

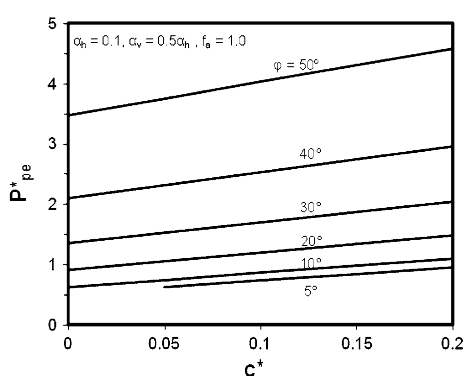

Fig. 3 Variation of nondimensional total passive force (P^*_{pe}) with nondimensional cohesion (c^*) for $\delta = 0.0$, $\alpha_h = 0.1$, $\alpha_v = 0.5\alpha_h$, $H/\lambda = 0.3$ and $H/\eta = 0.16$

Table 1 Values of (P^*_{pe}) for $f_a = 1.0$–2.0, $\varphi = 5°$–$50°$, $\delta = 0.0$, $c^* = 0.05$, $\alpha_h = 0.1$, $\alpha_v = 0$, $H/\lambda = 0.3$ and $H/\eta = 0.16$

f_a	φ (degree)					
	5	10	20	30	40	50
1.0	0.648	0.771	1.095	1.593	2.415	3.923
1.2	0.638	0.762	1.086	1.582	2.402	3.906
1.4	0.628	0.753	1.076	1.570	2.388	3.889
1.6	0.617	0.743	1.066	1.559	2.374	3.871
1.8	0.605	0.733	1.056	1.547	2.360	3.854
2.0	0.591	0.723	1.046	1.536	2.346	3.836

Table 1 shows the influence of amplification factor (f_a) on the nondimensional total passive force (P^*_{pe}) for $\varphi = 5°$–$50°$, $\delta = 0.0$, $c^* = 0.05$, $\alpha_h = 0.1$, $\alpha_v = 0$, $H/\lambda = 0.3$ and $H/\eta = 0.16$. It is noticed that P^*_{pe} decreases very slightly with increase in amplification factor (f_a). In other words, the effect of f_a on nondimensional total passive force (P^*_{pe}) is negligible compared to the effect of other parameters such as φ, c, α_h and α_v. The effect of wall friction angle (δ) on P^*_{pe} is presented in Table 2 for $\varphi = 20°$, $30°$, $\delta = 0.0$, 0.5φ, φ, $c^* = 0.00$–0.20, $\alpha_h = 0.0$, 0.1, 0.2, $\alpha_v = 0.5\alpha_h$, $H/\lambda = 0.3$ and $H/\eta = 0.16$. It is observed that, as expected, in all cases the wall friction angle has an increasing effect on P^*_{pe}. Choudhury and Nimbalkar (2005) observed the similar results for the specific case of $c = 0$. Table 3 shows the effect of variations in values of nondimensional parameters H/λ and H/η on P^*_{pe} for $\varphi = 20°$, $30°$, $\delta = 0.5\varphi$, $c^* = 0.05$, $\alpha_h = 0.1$–0.4, and $\alpha_v = 0.5\alpha_h$. It is seen that the magnitude of total passive force increases with increase in H/λ and H/η, i.e., by increase in the velocity of primary and shear waves, the magnitude of P^*_{pe} decreases. It is a significant finding that demonstrates the superiority of pseudo-dynamic method over pseudo-static method.

Figure 4 shows the variation of failure plane inclination angle with the horizontal plane (α) with seismic horizontal coefficient (α_h) for $a_v = 0$, $0.5a_h$, a_h, $\varphi = 10°$, $30°$, $50°$, $\delta = 0.0$, $c^* = 0.05$, $H/\lambda = 0.3$ and $H/\eta = 0.16$. It is seen that (1) the inclination angle (α) is lower for greater values of φ; (2) both the horizontal seismic coefficient (a_h) and vertical seismic coefficient (a_v) have decreasing effect on angle (α). Figure 4 also shows that the rate of decrease in angle (α) with respect to a_h is much more considerable for lower friction angles. For example, for $a_h = 0.2$ and $a_v = 0$ the value of α (in degrees) is

Table 2 Effect of wall friction angle (δ) on P^*_{pe} ($f_a = 1.0$, $\alpha_v = 0.5\alpha_h$, $H/\lambda = 0.3$ and $H/\eta = 0.16$)

φ	δ	α_h	P^*_{pe}				
			$c^* = 0.00$	$c^* = 0.05$	$c^* = 0.10$	$c^* = 0.15$	$c^* = 0.20$
20°	0	0	–	1.163	1.305	1.448	1.591
		0.1	0.907	1.051	1.194	1.337	1.480
		0.2	0.784	0.932	1.077	1.222	1.366
	0.5 φ	0	1.318	1.541	1.765	1.988	2.212
		0.1	1.145	1.370	1.594	1.818	2.042
		0.2	0.959	1.189	1.416	1.642	1.867
	φ	0	1.762	2.100	2.439	2.777	3.115
		0.1	1.500	1.839	2.178	2.516	2.855
		0.2	1.219	1.566	1.909	2.249	2.589
30°	0	0	–	1.673	1.846	2.020	2.193
		0.1	1.353	1.527	1.700	1.873	2.047
		0.2	1.200	1.376	1.550	1.724	1.898
	0.5 φ	0	2.488	2.832	3.178	3.522	3.867
		0.1	2.193	2.538	2.883	3.227	3.572
		0.2	1.889	2.236	2.582	2.928	3.274
	φ	0	3.053	3.493	3.933	4.373	4.813
		0.1	2.669	3.110	3.551	3.991	4.431
		0.2	2.278	2.721	3.162	3.604	4.045

Table 3 Effect of variations of H/λ and H/η values on P^*_{pe} ($f_a = 1.0$, $\alpha_v = 0.5\alpha_h$, $\delta = 0.5\ \varphi$, $c^* = 0.05$)

φ	α_h	P^*_{pe}			
		$H/\lambda = 0.3$	$H/\lambda = 0.4$	$H/\lambda = 0.5$	$H/\lambda = 0.6$
20°	0.1	1.370	1.385	1.404	1.425
	0.2	1.189	1.222	1.262	1.305
	0.3	0.991	1.047	1.111	1.180
	0.4	0.744	0.843	0.945	1.048
30°	0.1	2.538	2.564	2.595	2.631
	0.2	2.236	2.290	2.354	2.426
	0.3	1.925	2.009	2.109	2.219
	0.4	1.597	1.716	1.856	2.007

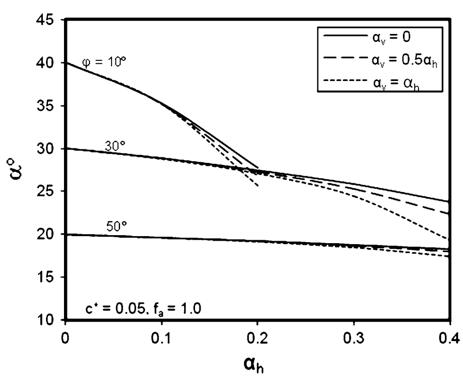

Fig. 4 Variation of failure plane inclination angle (α) with seismic horizontal coefficient (α_h) for $\varphi = 10°$, $30°$, $50°$, $\delta = 0.0$, $c^* = 0.05$, $H/\lambda = 0.3$ and $H/\eta = 0.16$

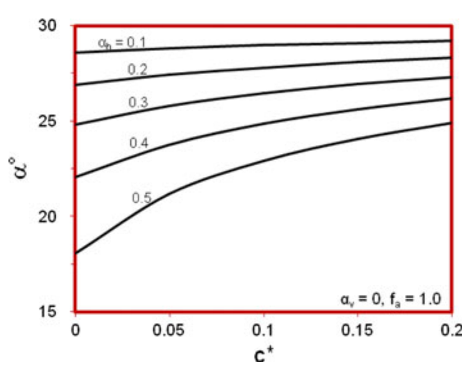

Fig. 5 Influence of nondimensional cohesion (c^*) on failure plane inclination angle (α) for $\varphi = 30°$, $\delta = 0.0$, $\alpha_v = 0.0$, $H/\lambda = 0.3$ and $H/\eta = 0.16$

69% of its static value for $\varphi = 10°$, whereas for $\varphi = 50°$ and the same set of parameters, α (in degrees) is just about 96% of its static value.

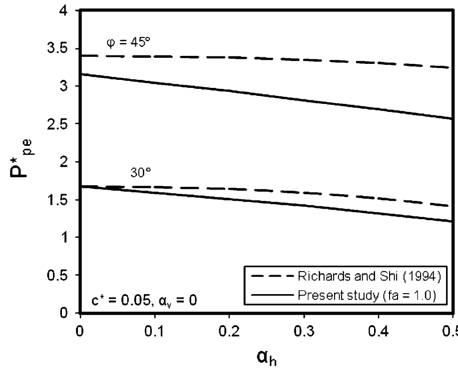

Fig. 6 Comparison of variation of nondimensional total passive force (P^*_{pe}) with horizontal seismic coefficient (a_h) obtained by the present study with earlier investigations

The influence of nondimensional cohesion (c^*) on failure plane inclination angle (α) is clearly shown in Fig. 5 for various values of horizontal seismic coefficient (a_h). It is observed that the angle (α) increases with increase in c^*, i.e., the area of the failure zone decreases. The reason seems to be due to the fact that the increase in backfill cohesion enhances the shear resistance of the backfill soil. Thus, the smaller portion of the backfill soil is subjected to collapse. The rate of the increase in angle (α) is much more considerable for higher values of a_h and lower values of c^*. For example, the value of α for $c^* = 0.2$ is 6.8° greater than $c^* = 0.0$ when $a_h = 0.5$; whereas it is just as small as 0.6° greater when $a_h = 0.1$ for the same values of c^*.

5 Comparison of Results

Fig. 6 shows the variation of P^*_{pe} with horizontal seismic coefficient (a_h) for $\varphi = 30°, 45°$, $\delta = 0.0$, $c^* = 0.05$, $\alpha_v = 0.0$, $H/\lambda = 0.3$ and $H/\eta = 0.16$ obtained by the present study compared to the results of Richards and Shi (1994). It is noticed that the results of present study propose the lower results. i.e., the present study is more conservative than Richards and Shi (1994) solution. Figure 6 also depicts that for higher values of a_h, the difference between present study and those of Richards and Shi (1994) increases.

6 Conclusions

The pseudo-dynamic approach was used to compute seismic passive earth thrust on the retaining walls with cohesive-frictional backfills. It is possible to consider time-dependent nature of earthquake acceleration in this method. The slip surface behind the wall was assumed to be planar. The results of present analysis shows that the total passive force (P^*_{pe}) decreases with increase in both horizontal seismic coefficient (α_h) and vertical seismic coefficient (α_v). The influence of α_v is more significant for higher values of α_h; the backfill cohesion has an increasing effect on P^*_{pe}; the effect of amplification factor (f_a) on nondimensional total passive force (P^*_{pe}) is negligible; the wall friction angle has an increasing effect on P^*_{pe}; by increase in the velocity of primary and shear waves, the magnitude of P^*_{pe} decreases; the inclination angle (α) is lower for greater values of φ and both the horizontal seismic coefficient (a_h) and vertical seismic coefficient (a_v) have decreasing effect on angle (α); the angle (α) increases with increase in backfill cohesion. The rate of this increase is much more considerable for higher values of a_h and lower values of cohesion. The comparison of results of present study with the results of earlier study shows the similar trend of total passive force variations with available parameters.

References

Choudhury D, Nimbalkar SS (2005) Seismic passive resistance by pseudo-dynamic method. Geotechnique 55(9):699–702

Choudhury D, Nimbalkar SS (2007) Seismic rotational displacement of gravity walls by pseudo-dynamic method: passive case. Soil Dyn EQ Engrg 27(3):242–249

Das BM (1993) Principles of soil dynamics. PWS-KENT Publishing Company, Boston

Ghahramani A, Anvar SA (2004) Dynamic earth pressure simulation by single degree of freedom system. Proceedings, 13th World Conf EQ Engrg, Vancouver

Kumar J (2001) Seismic passive earth pressure coefficients for sand. Can Geotech J 38(4):876–881

Mononobe N, Matsuo H (1929) On the determination of earth pressures during earthquakes, Proceedings, World Engr. Conf 9, Tokyo: 274–280

Okabe S (1926) General theory of earth pressure. J Japanese Soc Civ Eng Tokyo Japan 12(1)

Richards R, Shi X (1994) Seismic lateral pressures in soils with cohesion. J Geotech Eng ASCE 120(7):1230–1251

Saran S, Gupta RP (2003) Seismic earth pressures behind retaining walls.Indian Geotech J 33(3): 195-213

Saran S, Prakash S (1968) Dimensionless parameters for static and dynamic earth pressures behind retaining walls. Indian Geotech J 7(3):295–310

Soubra AH (2000) Static and seismic passive earth pressure coefficients on rigid retaining structures. Can Geotech J 37(2):463–478

Steedman RS, Zeng X (1990) The influence of phase on the calculation of pseudo-static earth pressure on a retaining wall. Geotechnique 40(1):103–112